DSMC simulations of turbulent flows at moderate Reynolds numbers

Cite as: AIP Conference Proceedings **2132**, 070010 (2019); https://doi.org/10.1063/1.5119564
Published Online: 05 August 2019

M. A. Gallis, J. R. Torczynski, N. P. Bitter, T. P. Koehler, S. G. Moore, S. J. Plimpton, and G. Papadakis

DSMC Simulations of Turbulent Flows at Moderate Reynolds Numbers

M. A. Gallis,[1,a)] J. R. Torczynski,[1,b)] N. P. Bitter,[1,c)] T. P. Koehler,[1,d)]
S. G. Moore,[2,e)] S. J. Plimpton,[2,f)] G. Papadakis[3,g)]

[1]*Engineering Sciences Center, Sandia National Laboratories,*
P. O. Box 5800, Albuquerque, New Mexico 87185-0840 USA
[2]*Computing Research Center, Sandia National Laboratories,*
P. O. Box 5800, Albuquerque, New Mexico 87185-1316 USA
[3]*Imperial College London, South Kensington Campus,*
London SW7 2AZ, UK

[a)]Corresponding author: magalli@sandia.gov; [b)]jrtorcz@sandia.gov, [c)]nbitter@sandia.gov,
[d)]tkoehle@sandia.gov, [e)]stamoor@sandia.gov, [f)]sjplimp@sandia.gov, [g)]g.papadakis@imperial.ac.uk

Abstract. The Direct Simulation Monte Carlo (DSMC) method has been used for more than 50 years to simulate rarefied gases. The advent of modern supercomputers has brought higher-density near-continuum flows within range. This in turn has revived the debate as to whether the Boltzmann equation, which assumes molecular chaos, can be used to simulate continuum flows when they become turbulent. In an effort to settle this debate, two canonical turbulent flows are examined, and the results are compared to available continuum theoretical and numerical results for the Navier-Stokes equations.

INTRODUCTION

The Direct Simulation Monte Carlo (DSMC) method was developed over 50 years ago by Graeme A. Bird[1] and is now a well-established statistical particle technique for modeling low-density gas flows. Recent advances in supercomputing technology (currently approaching the exascale level) have brought higher-density near-continuum flows within reach. However, at higher densities, the Reynolds numbers can become large enough for the flows to be in the turbulent regime. The ability of the Boltzmann equation (BE) and of DSMC to represent turbulent flow has been questioned and debated[2-5]. The source of this controversy is an assumption inherent in the derivation of the BE: molecular chaos. Some researchers[2,3] have suggested that molecular chaos globally eliminates correlations throughout the gas and thus is not compatible with the long-range velocity correlations that are needed to establish turbulent flow. Other researchers[4,5] have suggested that molecular chaos applies only at the molecular level (for collisions) and thus does not preclude the BE and DSMC from representing turbulent flows. Herein, we attempt to settle this debate by performing DSMC molecular-level simulations of two canonical incompressible turbulent flows studied extensively by many investigators and comparing the DSMC results to continuum-level computational and theoretical results from the Navier-Stokes equations (NSEs).

TAYLOR-GREEN FLOW

The first canonical turbulent flow examined is Taylor-Green (TG) vortex flow[6,7]. TG flow is a canonical turbulent flow in which the generation of small-scale eddies and the corresponding cascade of energy from small to large wavenumbers can be observed numerically. TG flow is initialized in a triply periodic domain $-\pi L \le \{x, y, z\} \le \pi L$ using velocity and pressure fields having only a single length scale L and a single velocity scale V_0:

31st International Symposium on Rarefied Gas Dynamics
AIP Conf. Proc. 2132, 070010-1–070010-6; https://doi.org/10.1063/1.5119564
Published by AIP Publishing. 978-0-7354-1874-5/$30.00

$$
\begin{aligned}
u &= V_0 \sin(x/L)\cos(y/L)\cos(z/L) \\
v &= -V_0 \cos(x/L)\sin(y/L)\cos(z/L) \\
w &= 0 \\
p &= p_0 + (\rho_0 V_0^2/16)(\cos(2x/L)+\cos(2y/L))(\cos(2z/L)+2)
\end{aligned}
\quad . \tag{1}
$$

Here, $\mathbf{u} = (u, v, w)$ is the velocity and p is the pressure at position $\mathbf{x} = (x, y, z)$ and time $T = 0$, where $T = V_0 t/L$. Thus, all of the kinetic energy is initially resident in a single wavenumber. Simulation results for the energy dissipation rate and the spectral energy distribution in TG flow are obtained for $\mathrm{Re} = 450$. Here, the Reynolds number is defined as $\mathrm{Re} = \rho V_0 L/\mu$, where ρ and μ are the gas density and the gas viscosity, respectively.

The DSMC code SPARTA[8] is used to simulate TG flow. SPARTA is an exascale-class open-source code capable of running efficiently on massively parallel, heterogeneous-architecture computational platforms. The computational domain is the cube defined by $-\pi L \le \{x, y, z\} \le \pi L$, where the domain length scale is $L = 0.0001$ m. This domain is subdivided into 8 billion cells (2000^3) with an average of 30 particles per cell for a total of 0.24 trillion particles. The time step is 3 ps. The gas has molecular mass $m = 46.5\times10^{-27}$ kg (nitrogen), specific heat ratio $\gamma = 5/3$ (internal energy disabled), and reference-property values at STP (101325 Pa, 273.15 K) for pressure, temperature, and density. The (maximum) velocity V_0 corresponds to a Mach number of 0.3, so the final temperature increase is roughly 1%. These conditions marginally satisfy the incompressibility assumption. The total physical time simulated is 18 μs.

Molecular collisions are performed using the Variable Soft Sphere (VSS) model[1]. To improve the spatial discretization, collision partners are selected from within a sphere having a radius that equals the distance traveled by the particle during a time step[9]. Multiple collisions between the same molecules during the same time step are not allowed, in accord with molecular chaos for collisions. Based on DSMC simulations of the two-dimensional analog to TG flow, this procedure yields a viscosity that leads to an effective Reynolds number of $\mathrm{Re} = 450$.

The DSMC results are compared to Direct Numerical Simulation (DNS) results from the spectral element code Nek5000[10]. The simulation domain is a cube with sides of length 2π, and the initial conditions are given by Eq. (1) with $V_0 = 1$. The fluid is incompressible with a constant density $\rho = 1$ and a constant viscosity $\mu = 1/\mathrm{Re}$. The simulation domain is discretized using 32 seventh-order spectral elements along each coordinate direction. Each spectral element contains 8^3 grid points placed at the Gauss-Lobatto nodes, for a total of 256 grid points along each coordinate axis. Third-order-accurate temporal integration is employed with a fixed Courant number of 0.8. After the simulation, the velocity fields are interpolated onto a uniform grid using the seventh-order polynomials associated with the spectral elements as interpolants. After interpolating the data onto this grid of equally-spaced points, discrete Fourier transforms are applied to obtain the energy spectra. To verify the DNS approach, the TG simulations of van Rees[11] at a Reynolds number of $\mathrm{Re} = 1600$ are reproduced. To confirm that the DNS results herein are mesh-independent, simulations are performed on 256^3 and 512^3 grids (i.e., 32 and 64 elements along each coordinate axis). The energy dissipation rates are found to differ by only 0.02% at $T = 9$ and by at most only 0.06% over $0 \le T \le 20$.

Figure 1 presents the u velocity component on the bounding planes of the domain from the DNS and DSMC simulations at $T = 9$, the time of maximum dissipation. Except for being slightly noisy, the DSMC molecular results are virtually identical to the DNS Navier-Stokes results. At the time of maximum dissipation, the large-scale structures that are the remnants of the initial conditions are clearly discernible, but smaller-scale structures are also present.

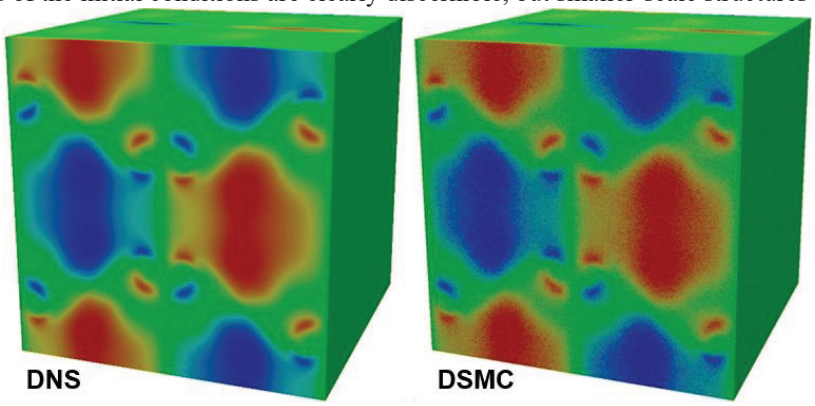

FIGURE 1. DNS and DSMC u velocity fields at $T = 9$ (maximum dissipation) have almost identical flow structures.

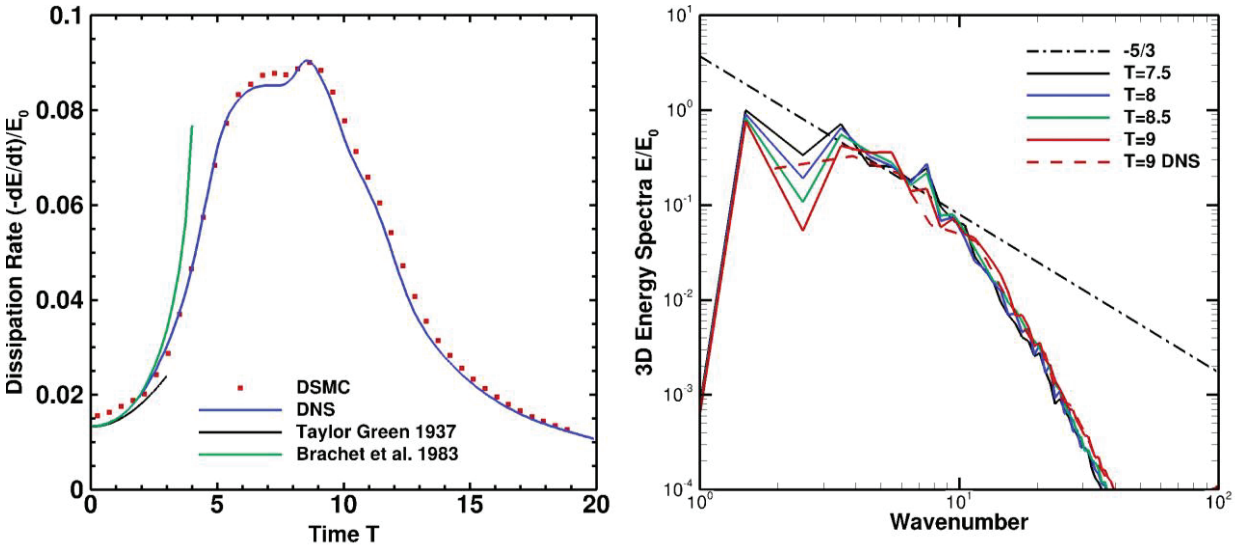

FIGURE 2. Left: energy dissipation rate as a function of time. Right: kinetic-energy spectra near maximum dissipation.

Figure 2 presents the DSMC and DNS energy dissipation rates as a function of time. The DSMC and DNS results are in good agreement over the entire time period during which the energy dissipation rate is significant. Both methods yield the same rapid increase from $T=2$ to $T=6$, the same plateau from $T=6$ to $T=8$, the same maximum between $T=8$ and $T=9$, the same rapid decrease from $T=9$ to $T=15$, and the same slow decrease from $T=15$ to $T=20$. DSMC does generally yield a slightly faster energy dissipation rate than DNS: the noticeably larger rate for $T\le 2$ may be caused by compressibility effects related to the finite initial Mach number (0.3). Results from the approximate viscous theory of Taylor and Green[6] and the approximate inviscid theory of Brachet et al.[7] are shown for comparison. Both theories are appropriate only for early times. For $2\le T\le 4$, these two approximate theories bracket the DSMC and DNS results.

Figure 2 also presents the DSMC and DNS three-dimensional kinetic-energy spectra at times near maximum dissipation. The DSMC spectra from $T=7.5$ to $T=9$ and the DNS spectrum at $T=9$ are in good agreement and both exhibit the Kolmogorov $-5/3$ law characteristic of turbulence over about 70% of a decade[12]. As time progresses, the kinetic energy in the low-wavenumber (large-wavelength) region of the spectrum decreases. During this time, energy is transferred from the initial large wavelength to smaller wavelengths, a process known as the energy cascade.

MINIMAL COUETTE FLOW

The second canonical turbulent flow examined is Minimal Couette Flow (MCF). As shown in Figure 3, MCF is a geometrically constrained three-dimensional Couette flow[13]. The domain is a rectangular cuboid bounded by walls on two opposite sides, and the origin of the coordinate system is located at the center of the cuboid. Its length in the x direction (streamwise) is $L_x=1.75\pi h$, its length in the z direction (spanwise) is $L_z=1.2\pi h$, and the corresponding pairs of boundaries are periodic. The walls are separated in the y direction (normal) by a distance $L_y=2h$ and slide in the x direction with tangential velocities $u_w=\pm V_0$. Typically, the no-slip boundary condition is applied on the walls so that $u=\pm V_0$ at $y=\pm h$, respectively. In the DSMC simulations, these walls are fully accommodating. A fully accommodating wall reflects the incident particles so that the reflected particles have a velocity distribution function in equilibrium with the wall velocity and temperature[1]. This boundary condition enforces impermeability but allows a nonzero slip velocity to exist between the wall and the gas in the presence of shear. When the mean free path λ is small relative to the gap half-height h (as is the case in this simulation), this slip velocity u_s is small compared to the wall velocity $u_w=V_0$. The normalized time and the Reynolds number are defined as $T=V_0t/h$ and $\mathrm{Re}=\rho V_0h/\mu$, where the gas has density ρ and viscosity μ.

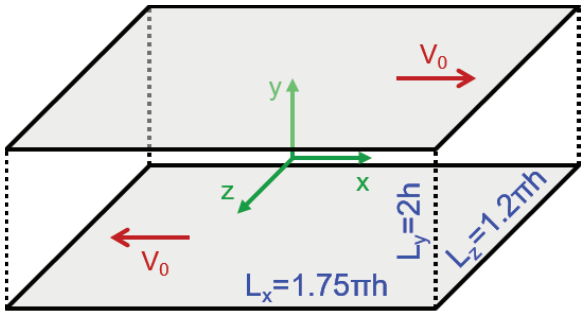

FIGURE 3. Minimal Couette Flow (MCF) physical domain.

The DSMC code SPARTA[8] is used to simulate MCF at $\mathrm{Re}=500$. The gap half-height is $h=500\ \mu$m, and the domain is divided into 1982×721×1359 cells (about 2 billion in total), which yields nearly cubical cells with a side length of $\Delta s=1.387\ \mu$m. Each of these cells has an average of 30 particles per cell (about 58 billion particles in total). Gas-molecule collisions are performed using the Hard Sphere (HS) collision model[1]. To improve spatial discretization, collision partners in a cell are selected from other particles within a sphere having a radius equal to the distance traveled by the particle during a time step[9]. The gas (argon) has molecular mass $m=66.3\times10^{-27}$ kg and specific heat ratio $\gamma=5/3$ and is initially at pressure $p_0=18190$ Pa and temperature $\theta_0=273.15$ K (the wall value), which yields a sound speed of $c_0=307.9$ m/s. A time step of $\Delta t=45.6$ ps is used, so particles move ~1% of the cell size Δs during each time step. The wall velocity $V_0=92.35$ m/s corresponds to a Mach number of 0.3, so the conditions marginally satisfy incompressibility. The domain length scale h has been selected to be large enough to establish continuum flow throughout the domain (small Knudsen layers) but small enough so that the simulation is tractable.

Discretization errors in DSMC increase the effective transport properties[14]. For these simulations, the effective viscosity μ and hence the effective Reynolds number Re are determined by comparing a one-dimensional DSMC simulation of laminar Couette flow (the domain is a single column of three-dimensional cells in the y direction) to the analytical expression for the wall shear stress of laminar Couette flow ($\tau=\mu V_0/h$). This comparison indicates that the discretization used for these simulations leads to an effective Reynolds number of $\mathrm{Re}=500$.

The gas has an initial velocity field that is the sum of a laminar Couette flow ($u=V_0y/h$) plus a sinusoidal perturbation applied throughout the domain. A perturbation is needed to enable MCF to become turbulent because linear stability theory indicates that laminar Couette flow is stable for all Reynolds numbers[13]. In agreement with linear stability theory, DSMC simulations initialized with only the unperturbed laminar profile stay laminar until the simulations are terminated (at $T=100$).

To assess the accuracy of the DSMC results, DNS simulations are performed using the spectral element code Nek5000[10], which has previously been shown to accurately simulate published results for turbulent Couette flow[15]. The fluid is continuum, incompressible, and isothermal. The DNS domain is discretized using 32 seventh-order spectral elements along each coordinate direction, with each element containing 8^3 grid points at the Gauss-Lobatto nodes, for a total of 256 grid points along each side of the domain. To confirm mesh independence, the simulations are repeated with 192 and 320 grid points along each coordinate axis, with no significant changes observed in the turbulence statistics (e.g., Reynolds stresses change by less than 2%). The DNS simulations are initialized with the same initial conditions used in the DSMC simulations. To ensure sampling statistics from a fully turbulent flow field, the DNS simulation is run without sampling until $T=200$ and then run with sampling up to $T=3000$. Convergence of the turbulence statistics is quantified by monitoring the profile of average shear stress through the channel, which is constant for statistically converged turbulent Couette flow. Here, the average shear stress profile differs from a constant by less than 0.6% across the channel, indicating sufficient sampling.

Figure 4 presents DSMC profiles of the streamwise velocity component u on the midplane between the sliding walls ($y=0$) at 27 consecutive times for MCF. The first profile is at time $T=267.408$, and adjacent profiles are separated by a time increment of $\Delta T=8.422$. Two vortices of opposite sense that are oriented predominantly in the streamwise direction are present. These vortices have diameters comparable to the gap height $2h$, so two vortices fit well into the spanwise extent of the domain since $L_z\approx 2L_y$. As time progresses, these vortices pass through several cycles of regeneration and decay: the vortices are disrupted significantly in Profiles 4, 8, 12, 16, and 20, and additional vortices appear transiently in Profiles 18, 21, 22, and 26. This continuous cycle of regeneration and decay sustains the turbulence in this flow.

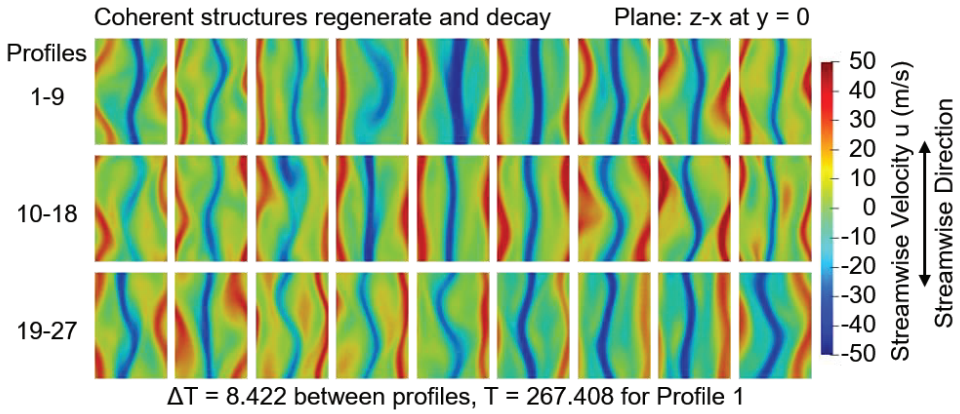

FIGURE 4. DSMC MCF streamwise velocity profiles on midplane between walls show sustained turbulence with several cycles of regeneration and decay of coherent structures.

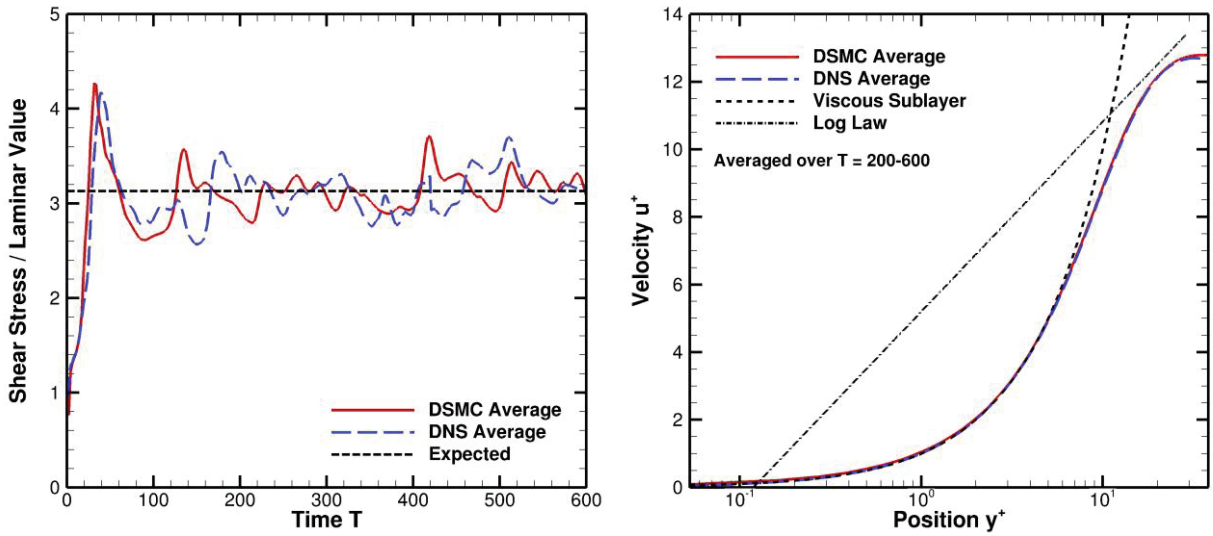

FIGURE 5. DSMC and DNS MCF results. Left: shear stress averaged over both walls. Right: law of the wall.

Figure 5 presents the shear stress (averaged over both walls) versus time from the DSMC and DNS simulations. The turbulent values are normalized by their laminar values: $\tau_{\text{lam}} = \mu V_0 / h$. Over the time interval of $T = 200\text{-}600$, the DSMC simulation yields a normalized shear stress of 3.13 ± 0.18, which agrees closely with the corresponding DNS value of 3.13 ± 0.20 (if the DNS averaging duration is increased to $T = 200\text{-}3000$, the expected value is unchanged). The DSMC simulation yields a normalized kinetic energy (not plotted herein) of 0.449 ± 0.048, which agrees closely with the DNS value of 0.449 ± 0.047. Although not identical in detail because turbulent flow is chaotic, the DSMC and DNS fluctuations have similar magnitudes and durations[16].

Figure 5 also presents the mean velocity profiles from the DSMC and DNS simulations. These profiles are found by averaging the streamwise velocity component u over times $T = 200\text{-}600$ and over the streamwise and spanwise coordinates x and z at each fixed value of the normal coordinate y. The resulting profiles are plotted using standard wall-based quantities: position $y^+ = \hat{y} v^* / \nu$ and velocity $u^+ = \hat{u} / v^*$, where $v^* = \sqrt{\tau_w / \rho}$, $\hat{y} = |y_w - y|$, $\hat{u} = |u_w - u|$, $y_w = \pm h$, $u_w = \pm V_0$, and τ_w is the average wall shear stress. The profiles from both walls are nearly identical, so their average is presented. The DSMC and DNS mean velocity profiles are almost identical and agree closely with the inner law $u^+ = y^+$ in the viscous sublayer ($y^+ < 8$). The log law $u^+ = (1/\kappa) \ln y^+ + B$ with $\kappa = 0.41$ and $B = 5.1$ is plotted for comparison. The DSMC and DNS mean velocity profiles approach the log law from below near $y^+ = 20$, but the Reynolds number $\text{Re} = 500$ is too low for the log law to be observed over a large portion of the domain. Although the DNS profiles exactly satisfy the no-slip condition at the walls, the DSMC profiles have a slip velocity of $u_s \approx 0.5$ m/s, which is small relative to the wall velocity of $V_0 = 92.35$ m/s and thus not dynamically significant.

CONCLUSIONS

The many aspects of agreement between the DSMC and DNS results indicate that the nonlinear regeneration processes in gas-kinetic methods (e.g., the BE) and continuum methods (e.g., the NSEs) are basically the same. The fact that the DSMC and DNS results agree closely for both the TG and MCF flows indicates that gas-kinetic methods like DSMC and, by extension, the BE that enforce molecular chaos only for gas-molecule collisions can indeed be used for quantitative investigations of turbulence. This conclusion is of significance to gas-kinetic theory because the assumption of molecular chaos for gas-molecule collisions plays key roles in derivations of the BE and of gas-kinetic molecular methods like DSMC. Additionally, DSMC can complement DNS because phenomena such as thermal relaxation and chemical reactions can be incorporated into DSMC at the molecular level in a straightforward manner. As supercomputing technology continues to advance, even larger Reynolds numbers will come within reach of DSMC.

ACKNOWLEDGMENTS

Sandia National Laboratories is a multimission laboratory managed and operated by National Technology and Engineering Solutions of Sandia, LLC, a wholly owned subsidiary of Honeywell International, Inc., for the U.S. Department of Energy's National Nuclear Security Administration under contract DE-NA0003525. This paper describes objective technical results and analysis. Any subjective views or opinions that might be expressed in the paper do not necessarily represent the views of the U.S. Department of Energy or the United States Government. This manuscript has been authored by National Technology and Engineering Solutions of Sandia, LLC, under Contract No. DE-NA0003525 with the U.S. Department of Energy. The United States Government retains and the publisher, by accepting the article for publication, acknowledges that the United States Government retains a non-exclusive, paid-up, irrevocable, world-wide license to publish or reproduce the published form of this manuscript, or allow others to do so, for United States Government purposes. J. R. Clausen, S. P. Kearney, and E. S. Piekos, Sandia National Laboratories, are thanked for providing insightful comments during the preparation of this paper.

REFERENCES

1. G. A. Bird, Molecular Gas Dynamics and the Direct Simulation of Gas Flows (Clarendon Press, Oxford, 1998).
2. H. Grad, J. Chem. Phys. 33 (5), 1342 (1960).
3. S. Tsugé, Phys. Fluids 17 (1), 22 (1974).
4. M. N. Kogan, Rarefied Gas Dynamics (Plenum Press, New York, 1969).
5. V. V. Aristov, Direct Methods for Solving the Boltzmann Equation and Study of Nonequilibrium Flows (Springer, New York, 2001).
6. G. I. Taylor and A. E. Green, Proc. Royal Soc. Lon. 158 (895), 499 (1937).
7. M. E. Brachet, D. I. Meiron, S. A. Orszag, B. G. Nickel, R. H. Morf, and U. Frisch, J. Fluid Mech. 130, 411 (1983).
8. S. J. Plimpton and M. A. Gallis, "SPARTA Direct Simulation Monte Carlo (DSMC) Simulator," http://sparta.sandia.gov (2015).
9. G. A. Bird, M. A. Gallis, J. R. Torczynski, and D. J. Rader, Phys. Fluids 21 (1), 017103, 1 (2009).
10. P. F. Fischer and J. W. Lottes, in Domain Decomposition Methods in Science and Engineering, Lecture Notes in Computational Science and Engineering 40, T. J. Barth et al., Ed., Berlin (Springer, Berlin Heidelberg, 2005).
11. W. M. van Rees, A. Leonard, D. I. Pullin, and P. Koumoutsakos, J. Comput. Phys. 230 (05), 2794 (2011).
12. M. A. Gallis, T. P. Koehler, J. R. Torczynski, S. J. Plimpton, G. Papadakis, Phys. Rev. Lett. 118, 064501 (2017).
13. J. Jimenez and P. Moin, J. Fluid Mech. 225, 213 (1991).
14. D. J. Rader, M. A. Gallis, J. R. Torczynski, and W. Wagner, Phys. Fluids 18, 077102 (2006).
15. K. H. Bech, N. Tillmark, P. H. Alfredsson, and H. I. Andersson, J. Fluid Mech. 286, 291 (1995).
16. M. A. Gallis, J. R. Torczynski, N. P. Bitter, T. P. Koehler, S. J. Plimpton, and G. Papadakis, Phys. Rev. Fluids 3, 071402(R) (2018).